

On the Use of Sweeping Langmuir Probes in Cutting-Arc Plasmas—Part II: Interpretation of the Results

Leandro Prevosto, Héctor Kelly, and Fernando Minotti

Abstract—A semiempirical Langmuir probe model is introduced that is particularly adapted to high-energy-density cutting arcs, for which, as we have shown in Part I, the ion current collected by negatively biased probes shows no plateau in the ion branch of the current–voltage (I – V) probe characteristic, and the signal amplitude is independent of the probe radius. According to the model, the ion drag due to the high-velocity plasma flow around the probe limits the effectively collecting area to a small fraction of the probe surface. If, according to the experimental evidence, this fraction is made independent of the probe radius, then its value results proportional to the probe bias, and so no plateau is found, at least as long as the collecting area is less than (half) the probe surface, which happens only at rather high probe bias. The model requires the determination of the function relating the electric field (in the region between the unperturbed plasma and the space-charge sheath close to the probe) to the parameters of the problem. Dimensional analysis together with empirical information allow to restrict the form of this function to leave only an auxiliary dimensionless function, which can be argued to be practically constant and whose value can be determined between rather tight bounds. As an example, radial profiles of plasma temperature and density are obtained by applying the proposed model to the experimental values of a I – V probe characteristic obtained in Part I. The derived temperature profile is in good agreement with a previous published numerical simulation for a similar cutting torch.

Index Terms—Cutting arcs, Langmuir probes, plasma diagnostic.

I. INTRODUCTION

IT IS WELL known that the derivation of the plasma properties from Langmuir-probe measurements solely depends on the theoretical model with which the probe (I – V) characteristic is interpreted. Unfortunately, there is only a limited range of experimental conditions under which the theory is only moderately complicated, i.e., low-pressure plasmas (where the collisional mean free path of charged particles is greater than the characteristic length of the probe and the perturbed region

Manuscript received May 4, 2007; revised November 16, 2007. This work was supported in part by the University of Buenos Aires under Grants PID X111 and X106 and in part by the Consejo Nacional de Ciencias y Tecnología (CONICET) under Grant PIP 2239/99.

L. Prevosto is with the National Technological University, Venado Tuerto 2600, Santa Fe, Argentina.

H. Kelly and F. Minotti are with the Instituto de Física del Plasma, Departamento de Física, Facultad de Ciencias Exactas y Naturales, Universidad de Buenos Aires, 1428 Buenos Aires, Argentina (e-mail: kelly@tinfipl.flp.uba.ar; minotti@df.uba.ar).

Digital Object Identifier 10.1109/TPS.2007.914182

around it). This is the case for which Langmuir's theory is strictly valid [1].

In high-pressure plasmas, the situation is quite different. Much of the work on Langmuir probes consider collision-dominated space-charge sheath and flow velocities much less than the speed of plasma sound [2]–[8]. The degree of ionization of the plasma is implicitly assumed to be low (less or equal to 10^{-4}), e.g., flames.

Clements and Smy [3] showed that, in weakly ionized plasmas, with small probes at high bias, the space-charge sheath will penetrate through the diffusion layer which surrounds the probe, with the result that the dominant mechanism for the supply of ions to the probe (for a negatively biased probe) becomes the convection of ions into the sheath by the hydrodynamic flow of the plasma. Such mechanism yields a probe current which varies as the square root of the probe bias.

In strongly ionized plasmas, the space-charge sheath is well differentiated from the diffusion layer, and thus, the ion current outside the sheath is diffusive [9], [10]. Besides, the Debye length in the temperature range of interest is usually smaller than the smallest mean free path, and thus, the space-charge sheath is collisionless. The resulting current is nearly independent of the probe potential, which is screened off, and coincides with the ion saturation current. The theory of probes in thermal plasmas has the added complexity that the matching of the space-charge sheath to the adjacent quasi-neutral presheath is extremely difficult [11]–[17]. It can only be done if a kinetic approach is adopted for the so-called Knudsen layer, between the continuum presheath (the region that matches the probe and plasma potentials) and the collisionless sheath, which has not yet been done for probes.

The interpretations of probe signals best developed for flowing thermal plasmas are those based on much more simplified probe theories (through order of magnitude estimates) for the calculation of the ion saturation current, in order to estimate the charged-particle density in the undisturbed plasma [9]. Experimental data on ion saturation currents for weakly ionized plasmas and for probes of cylindrical and spherical shapes are available in the literature. However, the theoretical treatment of these data has not been general: Every author or group of authors used his own theory [18], [19].

Benilov and Rogov [9] presented a study to treat probe measurements (see [9, Table 1]) in the framework of a unified theoretical technique. The theory considers an electric probe immersed in a uniform plasma composed of three species:

neutral particles, single-charged positive ions, and electrons; neglecting volume ionization and recombination in the sheath region. Moreover, this theory assumes that the current-collecting surfaces for spherical or cylindrical probes in a cross plasma flow are semispheres or semicylinders, respectively. The authors show that, in the framework of this model, the normalized values of cylindrical and spherical probes saturation currents may be approximately considered as universal functions of the diffusive Peclet number. That analytical model describes most of the data in [9, Table 1] within an accuracy of a factor three. Note that the covered range includes both weakly and strongly ionized plasmas; however, the plasma flow velocity is always well less than the ion-sound velocity.

More recently, Benilov [10] presented a theoretical work on the use of the probe characteristic curve for the determination of the electron temperature in the undisturbed plasma. In his work, it is shown that, over a wide range of parameters of high-pressure flowing plasmas, the current drawn by a negative probe does not perturb the distribution of the charged-particle density, electron temperature, and the plasma potential beyond a thin space-charge sheath. Besides, a semilogarithmic plot of the dependence of the electron current on the probe potential is close to a straight line. The value of the electron temperature determined using the slope of this plot corresponds to the edge of the aforementioned sheath.

High-energy-density cutting arcs are characterized by high-pressures (atmospheric and above), high space-charge densities (up to 10^{24} m^{-3}), and high velocities (up to about 6000 ms^{-1}) [20], so that the plasma velocities are around one order of magnitude higher than the highest velocities reported in [9, Table 1]. Furthermore, the published Langmuir-probe theories used in the investigation of high-pressure thermal plasmas [9], [10] cannot describe the unexpected results related to the probe characteristic and to the collecting probe area reported in Part I, i.e., the lack of ion current saturation, and the independence of the collected current on the probe area found in a high-energy-density cutting arc. In this paper, we present a new semiempirical Langmuir-probe model to interpret the experimental results presented in Part I. The model can be employed to derive the radial profiles of the plasma temperature and density along the arc. As an example, a case corresponding to a 30-A oxygen cutting torch at 3.5 mm from the nozzle exit is presented and discussed.

II. SEMIEMPIRICAL LANGMUIR-PROBE MODEL

In what follows, we present a simplified model to explain the ion branch of the probe characteristic in a high-pressure high-velocity plasma. The boundary layer of a highly ionized high-pressure collision-dominated plasma (probe radius $R_p \gg$ collision mean free path of charged particles \gg electron Debye length λ_D) in contact with a negatively biased probe (probe potential about or below the plasma potential) can be split up in two conventionally different zones: 1) a collision-free positive space-charge zone with an extension of some λ_D (the ‘‘sheath’’) and 2) a collision-dominated quasi-neutral zone with a typical extension $L \gg \lambda_D$ (the ‘‘presheath’’).

In the diffusive approximation, the ion flux toward the probe surface in the presheath region is due to ambipolar diffusion [1], [9], [10]

$$\bar{\Gamma}_+ = -D_a \nabla n \quad (1)$$

where n is the local charged-particle density, and D_a is the ambipolar diffusion coefficient

$$D_a \equiv \frac{(T_h + T_e)D_{ia}D_{ea}}{T_h D_{ea} + T_e D_{ia}} \quad (2)$$

where T_e and T_h are the electron and heavy-particle temperature, respectively, and D_{ia} and D_{ea} are the diffusion coefficients of ions and electrons in a neutral gas, respectively. Assuming that the plasma is in (at least partial) thermodynamic equilibrium, i.e., $T_e \cong T_h = T$, and taking into account that D_{ia}/D_{ea} is on the order of $\sqrt{m_e/m_i}$ (where m_e and m_i are the electron and ion mass, respectively), one can drop the second term in the denominator of (2), thus giving $D_a \cong 2D_{ia}$. This diffusion coefficient is related to gas kinetic parameters by [21]

$$D_a \approx 2\frac{1}{3}\bar{v}_i \lambda_{ia} \quad (3)$$

where \bar{v}_i is the ion mean thermal velocity, and λ_{ia} is the ion mean free path for collisions between ions and neutrals, defined by $\lambda_{ia} \equiv 1/n_n \sigma_0$, where n_n is the neutral density and σ_0 is the elastic cross section, typically $\approx 5 \times 10^{-19} \text{ m}^2$ [21], [22].

Using (1), the ion current density carried by the diffusive flux toward the probe is given by

$$\bar{j} \approx -eD_a \nabla n \quad (4)$$

where e is the electron charge.

Note that, in the frame of Clements and Smy classification [2], [3], the ion-flux regime toward the probe surface is purely diffusive if $Pe(e(V_p - V_s)/kT)^2(\lambda_D/R_p)^2 \ll 1$, where $Pe \equiv uR_p/D_a$ is the diffusive Peclet number (sometimes called the electrical Reynolds number). The convective regime holds in the opposite case. Here, $(V_p - V_s)$, k , and u are the probe potential V_p measured with respect to the unperturbed plasma potential V_s , the Boltzmann’s constant, and the plasma flow velocity, respectively. For flow velocities on the order of the ion-sound velocity (see as follows) and for $V_p - V_s \approx 24 \text{ V}$ (see Part I) is $Pe(e(V_p - V_s)/kT)^2(\lambda_D/R_p)^2 < 10^{-2}$ in the temperature range of interest ($T > 10 \text{ kK}$), thus supporting the validity of a diffusive approximation.

If the probe is under a negative potential with respect to the undisturbed plasma (about or below the probe-floating potential), the electron flux to the probe is of the same order of magnitude as, or smaller than, the low ion flux. Therefore, oppositely directed, high-diffusion, and drift electronic fluxes balance each other out to yield a very small resultant-net electron flux, then $\bar{\Gamma}_e \cong 0$ [1]. Considering the Einstein relation $D_e/\mu_e = kT/e$, the radial diffusive velocity in the quasi-neutral region is given by

$$D_a \frac{|\nabla n|}{n} = D_a \frac{e}{kT} E \quad (5)$$

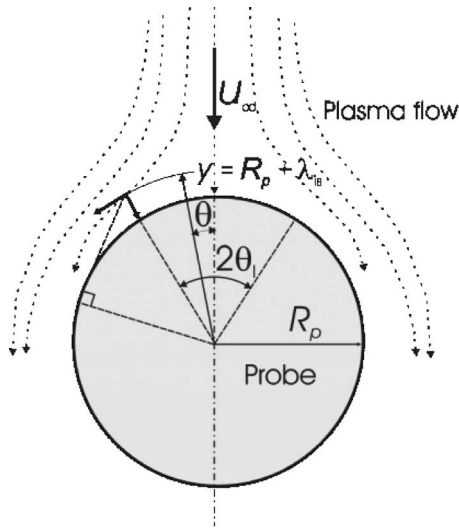


Fig. 1. Scheme of the probe and the plasma flow around it. The radius at which an average ion has its last collision with neutral before reaching the probe surface is indicated by y . The limiting condition at which this is possible is shown and the corresponding limit angle denoted by θ_1 .

where μ_e is the electron mobility, and E is the electric-field strength at the considered point.

Since a high-energy-density plasma cutting torch creates an underexpanded sonic flow at the nozzle exit [20], the arc-plasma jet velocity is on the order of the ion-sound velocity $v_{is} \equiv \sqrt{kT/m_i}$. For typical temperature values of an oxygen arc-plasma jet, $T \sim (1-2)10^4$ K, it results $v_{is} \sim (2-2.8)10^3$ ms⁻¹. Thus, the ions diffusing to the probe with a velocity forming a nonzero angle with the flow can be easily dragged by the plasma flow. If the flow is subsonic, in our case, photographs of the arc show the presence of a shock wave at $z \approx 1.1$ mm from the nozzle exit (where z is the axial coordinate along the arc), thus the flow is subsonic at distances larger than this value (and in particular for $z = 3.5$ mm); it can be modeled by the classical field velocity corresponding roughly to incompressible inviscid flow around a cylinder [23]. In the vicinities of the probe surface, the tangential velocity of this flow can be expressed as

$$u = u_\infty \left(1 + \left(\frac{R_p}{y} \right)^2 \right) \sin \theta \approx 2u_\infty \sin \theta \quad (6)$$

where y is the radius at the considered point, θ is the azimuthal angle measured from the upstream flow direction (see Fig. 1), and u_∞ is the unperturbed plasma flow velocity.

It has been suggested [9] that in atmospheric-pressure arc plasmas (flow velocity on the order of 10^2 ms⁻¹, corresponding to tungsten inert gas (TIG) arcs), only the front semicylinder of a cylindrical probe is active in charge collection. Other authors [19] have proposed that the active probe collecting area is controlled by the boundary-layer separation angle ($\approx 120^\circ$). Neither of these possibilities appears to describe our observed experimental behavior, i.e., the independency of the ion current on the probe radius.

The criterion suggested here is as follows. At the point of the last ion-neutral collision before the ions reach the probe,

$y \approx R_p + \lambda_{ia}$, the ion velocity [composed of the radial diffusive velocity in (5) and the tangential flow velocity in (6)] must be directed toward the probe surface if this ion is to reach that probe surface (see Fig. 1). This establishes a limit angle for the ion probe collection, which corresponds to an ion arriving tangentially at the probe surface. Using (5) and (6) and simple geometrical considerations, the value of the θ -limiting angle (θ_1) is given by

$$\sin \theta_1 \approx \frac{1}{2} \frac{D_a}{u_\infty} e \frac{E}{kT} \sqrt{\frac{R_p}{2\lambda_{ia}}}. \quad (7)$$

Using (4) and the Bohm criterion for a thin and collisionless sheath [11], the ion current density carried by the diffusive flux toward the probe, at $y = R_p + \lambda_D \cong R_p$, is given by

$$j \approx en_s v_B \quad (8)$$

where n_s is the charged-particle density at the sheath edge given by the approximate relationship $n_s \approx n_\infty / \sqrt{2.71}$ [1], [18], where the subscript ∞ denotes unperturbed values and $v_B \equiv \sqrt{kT/m_i}$ is the Bohm velocity, coincident with the ion-sound velocity. Note that the v_B value appearing in (8) refers to the value of this quantity at the border between the sheath and presheath regions. Since v_B is related to the electron temperature at the quoted border, we have estimated the electron-temperature perturbation, following Fanara's modification of the original Smy criterion for the occurrence of cooling [18]. The criterion compares the characteristic time (τ_f) during which the fluid is in contact with the cooling body (the probe), with the characteristic time (τ_e) for electron-energy losses. In Fanara's work, it is found that, for TIG arcs (with flow velocities around 100 m/s), the number of elastic collisions experienced during the characteristic time τ_f is as follows: $\tau_f \approx 10^5 \tau$ (where τ is the characteristic time for elastic collisions). Since, in a high-energy-density cutting arc, the flow characteristic velocity is around $2-3 \cdot 10^3$ m/s (sound velocity) and the characteristic time for electron-energy losses with oxygen atoms is around $3 \cdot 10^4$ times larger than the corresponding elastic-collision time (due to the smallness of the electron mass), it is obtained in our case $\tau_f \approx 0.2 \tau_e$, showing that the electron cooling is not relevant due to the high velocity flow.

It should be noted that, in practice, θ_1 is a small angle (the flow tangential velocity is much larger than the radial diffusive velocity at the point of the last collision), thus $2 \sin \theta_1 R_p \approx 2\theta_1 R_p$ represents the effective collecting area of the probe surface (per unit length). Using (3), (7), and (8), and taking the flow velocity as the ion-sound velocity, the ion-current per-unit length of the probe is given by

$$i'_p \approx 0.46 en_\infty v_B \lambda_{ia}^{1/2} \frac{eE}{kT} R_p^{3/2} \quad (9)$$

(all the numerical factors are embedded in the 0.46 number, including the ratio $\bar{v}_i/u_\infty = \sqrt{8/\pi}$).

In order to close the theory, the electric-field strength value must be related to the probe potential V_p , measured with respect to the unperturbed plasma potential V_s , and to the

intervening magnitudes of the problem, i.e., $E = f(|V_p - V_s|, \lambda_{ia}, R_p, T, m_i, u_\infty, n_\infty)$, the electron mass has been omitted because E is the field in the presheath region for the case $\lambda_D/R_p \rightarrow 0$ [11]. Dimensional analysis applied to this relation predicts that

$$E = \frac{|V_p - V_s|}{R_p} F\left(\lambda_{ia}/R_p, u_\infty/\sqrt{kT/m_i}, n_\infty \lambda_{ia}^3\right) \quad (10)$$

where F is a dimensionless function of its arguments.

Equations (9) and (10) predict, in general, a dependence of i'_p on R_p , but the experiment reported in Part I shows no such dependence. This fact determines the function F in (10) as $F(\xi) = \psi \xi^{1/2}$, with ψ a dimensionless function of $u_\infty/\sqrt{kT/m_i}$ and $n_\infty \lambda_{ia}^3$. With this expression for F , using (9) and (10), the ion-current per-unit length to the probe is given by

$$i'_p \approx 0.46 \psi e n_\infty v_B \lambda_{ia} \frac{e|V_p - V_s|}{kT}. \quad (11)$$

Equation (11) predicts an ion current that increases linearly with the absolute value of the probe-biasing voltage. The physical reason of this behavior is an increase of the probe collecting area as the probe bias increases as, from (7), θ_1 grows linearly with the E value (for a given value of R_p) and, thus, with $|V_p - V_s|$. A similar dependence between the probe current and the probe voltage can be seen in the experimental curve of Fig. 8 in Part I.

In order to relate the plasma potential V_s to the measured probe potential V_0 for zero-net current (see Part I), the following considerations are made. As the electron thermal velocity $\bar{v}_e \equiv \sqrt{8kT/(\pi m_e)}$ is very large as compared to the fluid-plasma velocity, the usual expression for the electron current collected by a probe applies. This current (per-unit probe length) for a cylindrical probe in a high-pressure plasma is [1]

$$i'_e = 2\pi R_p \frac{1}{4\gamma} n_\infty e \bar{v}_e \exp(-e|V_p - V_s|) \quad (12)$$

where the correction factor γ is given by

$$\gamma = 1 + \frac{\lambda_D}{2\lambda_{ea}} \frac{kT}{e(V_p - V_s)} \quad (13)$$

where λ_{ea} is the electron mean free path for collisions with neutrals. This factor γ is very close to unity for the conditions considered ($\lambda_D \ll \lambda_{ea}$ and $kT/e < |V_p - V_s|$), and so, we take $\gamma = 1$.

The V_0 value can be obtained equating (11) and (12) for $V_p = V_0$ to obtain

$$0.18 \psi \sqrt{\frac{m_e}{m_i}} \frac{\lambda_{ia}}{R_p} \frac{e|V_0 - V_s|}{kT} = \exp(-e|V_0 - V_s|). \quad (14)$$

This expression thus allows one to obtain V_s from the measured value of V_0 .

Equation (11) can be employed to derive information on the arc structure by using a geometrical inversion procedure. The geometry is shown in Fig. 2, which shows, at a given time, the probe axis passing through the arc section. Assuming circular symmetry for the arc profile, the arc core can be divided

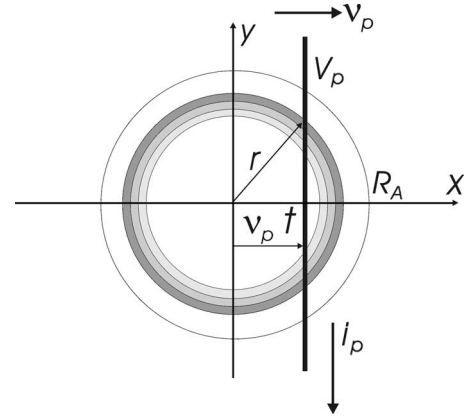


Fig. 2. Scheme of the probe sweeping across the plasma with velocity V_p used to obtain (12) for the Abel inversion. The plasma properties are supposed to vary with radial coordinate r , and so, each annulus of plasma at radius r contributes differently to the total probe current i_p , resulting in a time-dependent signal.

into several concentric elemental annulus so that the probe current can be expressed as the sum of contributions from many regions with different plasma properties but at the same probe potential. Using simple geometrical considerations, one can write from (11) the ion current in terms of an integral along the radial direction as follows:

$$i_p(x \equiv v_p t) = 2 \times 0.46 e \frac{|V_p(x) - V_s|}{k/e} \times \int_{r=|x|}^{R_A} \psi \frac{n_\infty v_B \lambda_{ia}}{T} \frac{r}{\sqrt{r^2 - x^2}} dr \quad (15)$$

where i_p is the total ion current (not per-unit length), x is the coordinate of the probe axis (determined by the probe velocity v_p at the time t , $x \equiv v_p t$), and R_A is the plasma-arc radius. By using the Abel-inversion technique, a radial profile of the plasma quantities can be derived from (15) with some additional assumptions, as the neutral density and the plasma density, and temperature are involved in the integral appearing in (15). These magnitudes can be related through the equation of state (assuming that the arc pressure is uniform along the radius) and through the Saha equation (local thermal equilibrium), thus closing the system. It is worth noting that the knowledge of the arc pressure is essential for the application of the presented procedure. This is the reason why the axial-probe positions must be taken after the characteristic shock front that appears close to the nozzle exit in this type of arcs, where the arc pressure can be considered to be the atmospheric value [20].

It is well known that any error in the input data for an Abel-inversion technique can be amplified in the computation, and care must be taken to reduce such errors to a minimum. To this end, the input data are fitted with a high-order polynomial before Abel inversion. The radial profile of temperature and plasma-charge density is then calculated in accord with the Saha equilibrium and the ideal gases equation for 0.13 MPa. The overpressure value of 0.03 MPa takes into account the stagnation effects in the upstream edge of the probe surface for a plasma flow velocity of $\approx 2 \times 10^{-3} \text{ ms}^{-1}$ (on the order of

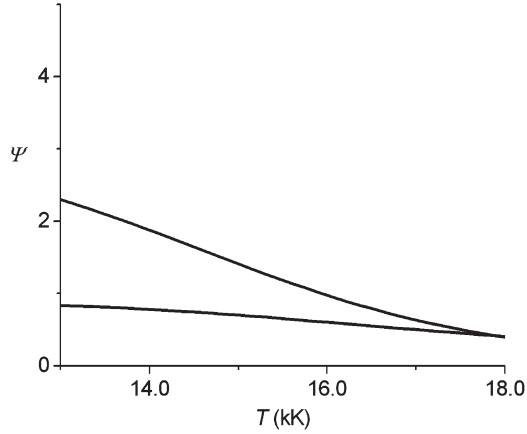


Fig. 3. Upper and lower bounds of the function ψ as a function of temperature.

the ion-sound velocity) and a plasma density corresponding to a pressure of 0.1 MPa and a temperature of 14 kK (as it will be shown in the next section, this is a typical value obtained for T).

Up to this point, the expression of the function ψ was left unspecified. It should be noted that a univocal determination of this function would require the complete solution of the sheath and presheath regions for collision-dominated highly ionized thermal plasmas flowing at velocities close to the sonic velocity. To our knowledge, this solution has not yet been determined. However, a determination of the admitted ψ values can be made by analyzing the bounds of the electric field in the presheath region. According to (10) and the expression of F , this field is given by

$$E = \psi \frac{|V_p - V_s|}{R_p} \sqrt{\frac{\lambda_{ia}}{R_p}}. \quad (16)$$

On the other hand, as $\sin \theta_1 \leq 1$, relation (7) determines that

$$E \leq 2 \frac{kT}{e} \frac{u_\infty}{D_a} \sqrt{\frac{2\lambda_{ia}}{R_p}} \quad (17)$$

while a lower bound can be obtained using as a potential difference across the presheath the conservative value kT/e and as a length scale the largest one, $L = R_p$, to obtain

$$\frac{kT}{eR_p} \leq E. \quad (18)$$

From (16), (18), one obtains

$$\frac{kT}{e|V_p - V_s|} \left(\frac{R_p}{\lambda_{ia}} \right)^{1/2} \leq \psi \leq 2\sqrt{2} \frac{kT}{e|V_p - V_s|} \frac{u_\infty}{D_a}. \quad (19)$$

The bounds in (19) can be evaluated as a function of T using the less favorable values, for each bound, of R_p and/or of $|V_p - V_s|$ used in the experiment reported in Part I. The results are shown in Fig. 3, where it can be appreciated that the allowed values of ψ are restricted to a rather narrowband around unity. This is very suggestive because the arguments of ψ are $u_\infty/\sqrt{kT/m_i}$ and $n_\infty\lambda_{ia}^3$. The first one is approximately unity, whereas the second one varies between $\approx 10^{17}$ and $\approx 2 \times 10^{18}$

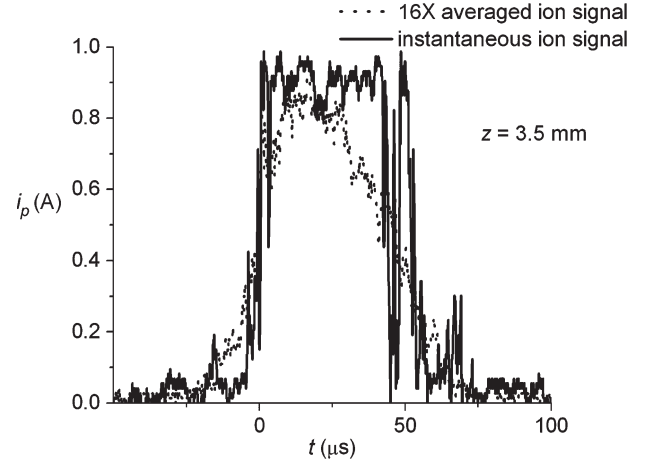


Fig. 4. Experimental ion-current signal for a probe sweeping across the arc at 3.5 mm from the nozzle exit of a 30-A oxygen cutting torch. Solid line: Instantaneous signal. Dashed line: Average over 16 successive instantaneous signals.

for the temperatures of interest. As no other dimensionless parameters exist of similar magnitude, a value of order unity for ψ can be obtained only if its dependence on $n_\infty\lambda_{ia}^3$ is extremely weak. This allows one to treat ψ as a constant (the value of $u_\infty/\sqrt{kT/m_i}$ is very close to unity in the region considered). As the value of ψ is limited by the largest value of the lower bound and the lowest value of the upper bound in the whole temperature range where the model applies ($\theta_1 \leq \pi/2$), one should take ψ very close to one. From (14), we thus obtain, for the temperature range of interest (12–16) kK and for $R_p = 63 \mu\text{m}$, that $V_s - V_0 \approx 8 \text{ V}$ with a slight dependence on R_p .

III. RESULTS OF THE INVERSION PROCEDURE

In Fig. 4, two ion-current signals are presented (one instantaneous and one 16 \times averaged) that will be used to perform the inversion procedure. The probe radius was $63 \mu\text{m}$, and the probe tangential velocity was 18 ms^{-1} in this example. The averaged signal represents an average over 16 consecutive instantaneous signals (this means that the average is performed over a time $\approx 1 \text{ ms}$). Note that the instantaneous signal presents an almost square shape, while the averaged one presents a Gaussian-like shape with a somewhat larger duration.

In Figs. 5 and 6, the obtained profiles of the plasma temperature and density, respectively, are shown corresponding to both ion-current signals. The chosen value for ψ was one in this case. As shown, the temperature profiles show a monotonic decreasing behavior from the arc center, with a peak value (T_0) somewhat higher for the instantaneous signal ($T_0 \approx 15 \text{ kK}$, whereas $T_0 \approx 14.2 \text{ kK}$ for the averaged signal). In addition, the instantaneous signal gives a thinner arc (the instantaneous profile decays abruptly at $\approx 0.6 \text{ mm}$, whereas corresponding to the averaged signal at $\approx 1.1 \text{ mm}$). It is worth noting that the abrupt decay at the end of the profiles cannot be taken with confidence as it is an artifact of the Abel-inversion technique. The reason was pointed out by Gick *et al.* [19] and is related to the fact that, for temperatures below about 6 kK, the function that is being inverted in (12) decays too fast with the temperature to give accurate values for this quantity. There are no

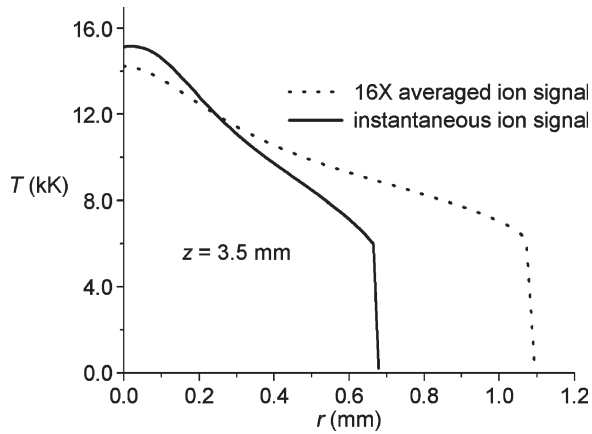


Fig. 5. Temperature of the plasma, as a function of the radial coordinate, obtained from the inversion of the instantaneous signal (solid line) and of the averaged signal (dashed line) shown in Fig. 4.

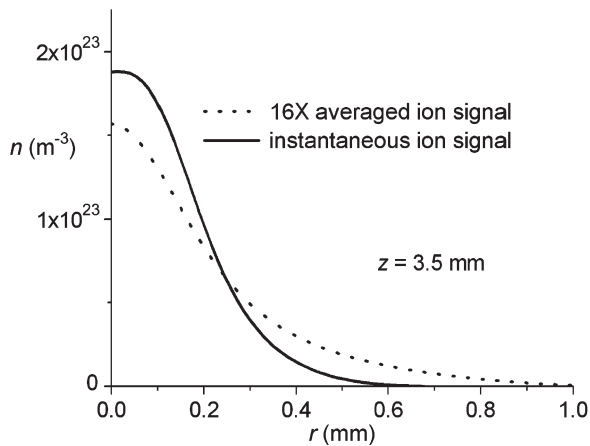


Fig. 6. Plasma-density radial profile corresponding to the temperature profile in Fig. 5.

experimental data available on temperature measurements for an arc of similar characteristics to those considered here, at the axial positions explored in this paper (spectroscopic temperature measurements in a similar arc have been presented but at an axial position very close to the nozzle exit [20]). However, there are numerical simulations, validated with experimental results, which predict temperature profiles that are very close to those obtained here at the same axial position [20]. Note that the electron temperature values inferred from the inversion procedure of (15) are in agreement with the previous estimation of low electron cooling.

The plasma-density profiles shown in Fig. 6 are obtained from the temperature profiles in Fig. 5 by applying the ideal gas law and Saha equation (at the constant pressure of 0.13 MPa). As expected, the profiles are concentrated in the region of high temperature ($T > 10$ kK), and correspondingly, the instantaneous peak value is higher than that of the averaged value. For both profiles, the plasma is located within a radius of ≈ 0.3 mm.

Concerning the uncertainty in the plasma-quantity profiles derived from the possible values of ψ , it should be mentioned that, within the allowed band shown in Fig. 3, the T_0 value

varies in less than 1 kK, and correspondingly, the peak-density value is affected by no more than 7%.

Since it was shown in Part I that, in these experiments, the arc voltage presented a strong ripple component, amounting to around 10% (peak value) with respect to the average dc component, a possible explanation of the relation between this fluctuations with the fluctuation experimentally observed in the amplitude and width of the ion-current signal ($< 10\%$ and 30% , respectively, see Part I) are in order. It has been shown by Pardo *et al.* [24] (using spectroscopic measurements in a cutting torch with a similar level of arc-voltage fluctuation) that a voltage fluctuation of 10% results in a similar level of fluctuation in the plasma temperature. In our case, it is clear that, since the period of the ripple signal (≈ 7 ms) is much larger than the transit time of the probe along the arc (≈ 50 μ s, when registering an ion-current signal), the whole detection time of the ion-current signal occurs under a practically constant value of the arc voltage (which, in principle, is somewhat unknown, varying in $\pm 10\%$ around the average voltage value).

From a physical point of view, if the arc voltage increases, an increase in the arc current is expected and a consequent increase in T . However, the behavior of n is somewhat more complicated. Since we are dealing with a region of free arc burning, the outer pressure (that approximately fixes the arc pressure) does not vary as the arc voltage changes; hence, it is easy to show that n grows strongly with T for relatively low T values (basically, due to a strong increase in the ionization degree), up to a maximum value for $T \approx 18$ kK (for an external pressure of 0.13 MPa, a typical value in the region of our measurements), and finally begins to decrease for larger T values because the first oxygen ionization has been almost completed. This behavior is translated to the arc structure in the following way: Since the arc T and n profiles present a central peak with values decaying to the arc border, a global increase in the arc temperature profile is not translated similarly to the n profile. The peak central value of n will change only a little (because the central arc T value is very close to that corresponding to the peak-density value, see Fig. 5), while the density values in the outer regions of the arc will strongly increase (due to an abrupt increase in the ionization degree in those regions). This behavior will result in a thicker ion-current signal. Note that the peak value of the ion signal does not change too much, because the variation of the plasma quantities in the central arc regions have not varied too much [and, in particular, the ion signal is strongly dependent on n but varies only with the square root of T , see (11)]. The situation for a lower arc-voltage value is completely similar, resulting in a thinner ion-current signal with almost the same amplitude.

In conclusion, we believe that the voltage ripple is causing the 30% and $< 10\%$ variations in the ion-signal width and ion-signal amplitude, respectively, that was experimentally observed.

For the above quoted reasons, the shape of the $16\times$ average arc quantities profiles presented in Figs. 5 and 6 are possibly distorted by the ripple frequency, but this is not the case in the derived profiles of the instantaneous signals. Note that these signals were registered at practically constant value of the arc voltage (temporal width ≈ 50 μ s \ll period of the ripple

signal ≈ 7 ms), and so, practically in absence of the voltage ripple.

IV. FINAL REMARKS

In this paper, we present a new semiempirical Langmuir-probe model to interpret the experimental results presented in Part I. Although semiempirical in character, the presented model allows a quantitative determination of plasma magnitudes from the ion I - V relation of a sweeping probe close to the nozzle exit of a high-energy-density cutting torch. This is possible because the unknown function ψ in (11) can be argued to have values between rather tight bounds (determined from the experimental results) to depend weakly on the value of $n_{\infty}\lambda_{ia}^3$, and also because, the plasma flow is close to the ion-sound velocity. The model can be employed to derive the radial profiles of the plasma temperature and density along the arc, using the Abel-inversion technique. The maximum uncertainty in the plasma-quantity profiles derived from the possible values of ψ is less than 1 kK for the axial temperature value, and correspondingly, the peak-plasma-density value is affected by no more than 7%. As an example, the application to measurements on a 30-A oxygen cutting torch at 3.5 mm from the nozzle exit was presented and discussed. The predicted temperature profile was in good agreement with a previously published numerical simulation for a similar cutting torch.

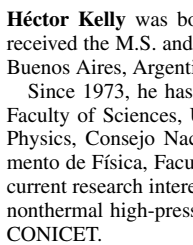
REFERENCES

- [1] Y. P. Raizer, *Gas Discharge Physics*. Berlin, Germany: Springer-Verlag, 1991.
- [2] R. M. Clements and P. R. Smy, "Ion saturation currents to planar Langmuir probes in a collision-dominated flowing plasma," *J. Phys. D, Appl. Phys.*, vol. 6, no. 2, pp. 184–195, Jan. 1973.
- [3] R. M. Clements and P. R. Smy, "Ion current from a collision-dominated flowing plasma to a cylindrical electrode surrounded by a thin sheath," *J. Appl. Phys.*, vol. 41, no. 9, pp. 3745–3749, Aug. 1970.
- [4] B. M. Oliver and R. M. Clements, "Sheath growth in a flowing high-pressure plasma," *J. Phys. D, Appl. Phys.*, vol. 8, no. 8, pp. 914–921, Jun. 1975.
- [5] R. M. Clements and P. R. Smy, "The floating potential of a Langmuir probe in a high-pressure plasma," *J. Phys. D, Appl. Phys.*, vol. 7, no. 4, pp. 551–562, Mar. 1974.
- [6] R. M. Clements, S. A. H. Rizvi, and P. R. Smy, "Langmuir probe characteristics in a high pressure plasma in the presence of convection and ionization," *IEEE Trans. Plasma Sci.*, vol. 22, no. 4, pp. 435–441, Aug. 1994.
- [7] R. M. Clements, B. M. Oliver, and P. R. Smy, "Pulsed spherical probe measurements of plasma conductivity in a flowing continuum plasma," *J. Phys. D, Appl. Phys.*, vol. 10, no. 16, pp. 2213–2224, Nov. 1977.
- [8] R. M. Clements and P. R. Smy, "Transition from diffusion-convection to sheath-convection of a cold Langmuir probe in a moving compressible plasma," *J. Phys. D, Appl. Phys.*, vol. 14, no. 6, pp. 1001–1008, Jun. 1981.
- [9] M. S. Benilov and B. V. Rogov, "Ion saturation currents to spherical and cylindrical electrostatic probes in collisional plasmas," *J. Appl. Phys.*, vol. 70, no. 11, pp. 6726–6731, Dec. 1991.
- [10] M. S. Benilov, "Can the temperature of electrons in a high-pressure plasma be determined by means of an electrostatic probe?" *J. Phys. D, Appl. Phys.*, vol. 33, no. 14, pp. 1683–1696, Jul. 2000.
- [11] K. U. Riemann, "The Bohm criterion and sheath formation," *J. Phys. D, Appl. Phys.*, vol. 24, no. 4, pp. 493–518, Apr. 1991.
- [12] K. U. Riemann, "Kinetic analysis of the collisional plasma-sheath transition," *J. Phys. D, Appl. Phys.*, vol. 36, no. 22, pp. 2811–2820, Nov. 2003.
- [13] H. Schmitz and K. U. Riemann, "Consistent analysis of the boundary layer of a Saha plasma," *J. Phys. D, Appl. Phys.*, vol. 34, no. 8, pp. 1193–1202, Apr. 2001.
- [14] R. N. Franklin, "Where is the 'sheath edge'?" *J. Phys. D, Appl. Phys.*, vol. 37, no. 9, pp. 1342–1345, May 2004.
- [15] R. N. Franklin, "There is no such thing as a collisionally modified Bohm criterion," *J. Phys. D, Appl. Phys.*, vol. 36, no. 22, pp. 2821–2824, Nov. 2003.
- [16] R. N. Franklin, "What significance does the Bohm criterion have in an active collisional plasma-sheath?" *J. Phys. D, Appl. Phys.*, vol. 35, no. 18, pp. 2270–2273, Sep. 2002.
- [17] R. N. Franklin, "The plasma-sheath boundary region," *J. Phys. D, Appl. Phys.*, vol. 36, no. 22, pp. R309–R320, Nov. 2003.
- [18] C. Fanara, "Sweeping electrostatic probes in atmospheric pressure arc plasmas—Part II: Temperature determination," *IEEE Trans. Plasma Sci.*, vol. 33, no. 3, pp. 1082–1092, Jun. 2005.
- [19] A. E. F. Gick, M. B. C. Quigley, and P. H. Richards, "The use of electrostatic probes to measure the temperature profiles of welding arcs," *J. Phys. D, Appl. Phys.*, vol. 6, no. 16, pp. 1941–1949, Oct. 1973.
- [20] P. Freton, J. J. Gonzalez, A. Gleizes, F. Camy Peyret, G. Caillibotte, and M. Delzenne, "Numerical and experimental study of a plasma cutting torch," *J. Phys. D, Appl. Phys.*, vol. 35, no. 2, pp. 115–131, Jan. 2002.
- [21] M. I. Boulos, P. Fauchais, and E. Pfender, *Thermal Plasmas*, vol. 1. New York: Plenum, 1994.
- [22] H. L. Anderson, *A Physicist's Desk Reference*, 2nd ed. New York: AIP, 1989.
- [23] L. D. Landau and E. M. Lifshitz, *Fluids mechanics*, vol. 6, Theoretical Physics Course, 1991. Reverté.
- [24] C. Pardo, J. González-Aguilar, A. Rodríguez-Yunta, and M. A. G. Calderón, "Spectroscopic analysis of an air plasma cutting torch," *J. Phys. D, Appl. Phys.*, vol. 32, no. 17, pp. 2181–2189, Sep. 1999.



Leandro Prevosto was born in Santa Fe, Argentina, on November 29, 1971. He received the degree in electromechanical engineering from the National Technological University, Venado Tuerto, Santa Fe, Argentina, in 2005.

Since 2006, he has been on a fellowship with the Fundación Yacimientos Petrolíferos Fiscales, Argentina, and has been conducting Ph.D. studies with the Institute of Plasma Physics, Consejo Nacional de Ciencias y Tecnología, Departamento de Física, Facultad de Ciencias Exactas y Naturales, Buenos Aires, Argentina, and the Engineering University of Buenos Aires.



Héctor Kelly was born in Mendoza, Argentina, on February 14, 1948. He received the M.S. and Ph.D. degrees in physics from Buenos Aires University, Buenos Aires, Argentina, in 1972 and 1979, respectively.

Since 1973, he has been a researcher with the Plasma Physics Laboratory, Faculty of Sciences, University of Buenos Aires, and the Institute of Plasma Physics, Consejo Nacional de Ciencias y Tecnología (CONICET), Departamento de Física, Facultad de Ciencias Exactas y Naturales, Buenos Aires. His current research interests are high-power electric discharges, vacuum arcs, and nonthermal high-pressure plasmas. Since 1980, he has been a researcher with CONICET.



Fernando Minotti was born in Buenos Aires, Argentina, on January 27, 1960. He received the degree in physics and the Ph.D. degree from the University of Buenos Aires, Buenos Aires, Argentina, in 1984 and 1990, respectively.

From 1991 to 1993, he held a Postdoctoral position with the Goddard Institute for Space Studies, National Aeronautics and Space Administration, NY. Since 1993, he has been a Researcher with the Consejo Nacional de Ciencias y Tecnología (CONICET), Argentina, and he has been working with the Institute of Plasma Physics, CONICET and the Universidad de Buenos Aires. Since 1998, he has been a Professor with the Universidad de Buenos Aires.